ELSEVIER

Contents lists available at ScienceDirect

Applied Catalysis A, General

journal homepage: www.elsevier.com/locate/apcata



MCM-41/ZSM-5 composite particles for the catalytic fast pyrolysis of biomass



Lei Yu^a, Azeem Farinmade^b, Oluwole Ajumobi^b, Yang Su^b, Vijay T. John^b, Julia A. Valla^{a,*}

- ^a Department of Chemical and Biomolecular Engineering, University of Connecticut, Storrs, 191 Auditorium Road, Unit 3222, CT 06269, USA
- ^b Department of Chemical & Biomolecular Engineering, Tulane University, 6823 St. Charles Avenue, New Orleans, LA 70118, USA

ARTICLE INFO

Keywords: Catalytic fast pyrolysis ZSM-5 MCM-41 Composite Catalyst deactivation

ABSTRACT

ZSM-5 is a promising catalyst for the catalytic fast pyrolysis (CFP) of biomass due to its high selectivity to light hydrocarbons. However, rapid deactivation of catalyst has been a major challenge towards the commercialization of CFP. The objective of our study is to evaluate the performance of MCM-41/ZSM-5 composites during the CFP of biomass. Here, for the first time, we report the synthesis of a unique MCM-41/ZSM-5 composite via a one-step, facile aerosol-based method. The composition of ZSM-5 in the composites was varied and the prepared composites were used as catalysts for the in-situ and ex-situ CFP of miscanthus \times gigantus. The prepared composites were characterized by N_2 adsorption-desorption, XRD, SEM, TEM and DRIFTS-pyridine adsorption. The results of CFP experiments demonstrated that ZSM-5 in the composites was fully accessible. Most importantly, MCM-41 acted as a sacrificial layer for coke deposition and decreased the deactivation rate of the ZSM-5.

1. Introduction

The production of fuels and energy *via* biomass pyrolysis has drawn significant scientific attention due to the low cost, renewability and sustainability of the resource [1–3]. The primary products of biomass pyrolysis are bio-oil, syngas and biochar. Bio-oil shows great potential to replace the traditional petroleum-based fuels. However, bio-oil is mainly composed of oxygenates, which are responsible for its undesired properties, such as high acidity and viscosity and low heating value [4]. Hence, the upgrading of pyrolysis bio-oil is necessary before its use. Catalytic fast pyrolysis (CFP) of biomass takes place at high heating rates in the presence of a catalyst [5,6]. During CFP the bio-oil is upgraded by removing oxygen and increasing the selectivity of hydrocarbons in bio-oil. The use of catalysts with high deoxygenation activity is key for the production of high quality bio-oil that is rich in hydrocarbons [7,8].

Numerous catalysts have been studied for the CFP of biomass over the past decades, such as zeolites (Y zeolite, beta-zeolite [9] and ZSM-5 [10–12]), silica (amorphous silica [13], SBA-15 [14] and MCM-41 [5]) and oxides (CaO, MgO [15], ZnO [16], γ -Al₂O₃ [17] and TiO₂ [18]). Research studies agree that ZSM-5 is one of the most effective catalysts owing to its acidity and unique shape and pore size, which favor deoxygenation reactions and the production of light aromatic hydrocarbons, such as benzene, toluene and xylene (BTX) [15,19,20].

However, one of the major drawbacks of ZSM-5 is the fast deactivation due to the coke formation. A number of studies have been conducted to understand the mechanism of coke deposition on ZSM-5 [6,21-24]. Researchers argue that since the kinetic diameter of large intermediate oxygenates is larger than the pore diameter of ZSM-5, the restricted mass transfer should result in the polymerization of large oxygenates on the external surface of zeolites, which can further block the inner microporous channels and deactivate the zeolite [25]. Gou et al. studied the effect of mesoporosity in ZSM-5 on the CFP of furan [19] and concluded that introducing mesopores into ZSM-5 improved the conversion of furan and the selectivity to aromatics and olefins, and largely reduced the coke formation. Hoff et al. [26] argued that external surface barriers played a minimal role on the deposition of coke, while micropore diffusion was the dominant contribution to the formation of coke. Yang et al. suggested that ZSM-5 could be deactivated by coke through both micropores filling and acid sites blocking [27]. Xu et al. also studied the effect of introducing mesoporosity in MFI zeolites through the formation of nanosheets [28]. and concluded that the later produced similar aromatic hydrocarbon yields and had longer lifetime compared to conventional HZSM-5. However, the MFI nanosheets showed high coke yield, which was attributed to the higher accessibility of active sites due to the extra space-volume created by mesopores. We previously [29] tested various MFI-type zeolites with varying degrees of mesoporosity and concluded that the highest yield of hydrocarbons and

E-mail address: ioulia.valla@uconn.edu (J.A. Valla).

^{*} Corresponding author.

minimum coke formation could be realized by optimizing mesopore size and zeolite acidity. Although significant discoveries have been made over the past years on the development of hierarchical ZSM-5 zeolites as a means to prevent coke formation in ZSM-5 and increase hydrocarbon selectivity during biomass CFP, the challenge still exists. On the top of this challenge, hydrothermal and mechanical stability are also significant factors for the lifetime of catalysts, especially those with mesopores.

Recently, the development of composites of ZSM-5 and mesoporous materials, such as MCM-41, SBA-15 and silicalite-1, as a means of combining the benefits of microporous acidic zeolites and mesoporous materials, has been investigated, with reported benefits [25,30-32]. The hypothesis is that when pyrolysis vapors pass through the coreshell structured catalyst, they first crack into smaller oxygenates in the mesoporous layer, and the formed smaller molecules can convert into hydrocarbons in the microporous core (ZSM-5). Hu et al. synthesized core-shell HZSM-5@silicalite-1 catalysts for biomass CFP [30]. The silicalite-1 was composed entirely of Si and O and was used to cover the external acid sites of HZSM-5 and minimize possible reactions on the external surface. Zou et al. also used hierarchical ZSM-5/MCM-41 catalyst for the CFP of co-pyrolysis of lignin and waste oil and observed excellent aromatization and bond-breaking abilities by the catalyst [33]. Other mesoporous materials, such as SBA-15 were also used to prepare core-shell structured catalysts [25]. Li et al. also prepared mesoporous ZSM-5 coated with thin microporous silicalite-1 and tested their catalytic performance on pine sawdust CFP [34] showing high hydrothermal stability of the catalyst and high selectivity to p-xylene.

In the CFP of biomass, large crystals of ZSM-5 possess significant diffusional restrictions for large molecules to access the interior acid sites. Submicron crystals of ZSM-5 may enable such access, but such microcrystals lead to high pressure drops in packed bed reactors and need to be integrated into porous support matrices. Thus, the concepts of integrating small crystals of the zeolite into an MCM-41 matrix has relevance both to reactor design and to product distributions. While procedures for building an MCM-41 shell around zeolite microcrystals to make core shell structures [25,30–32], or introducing mesoporosity in large crystals through selective etching are feasible, the procedures are complex and lead to difficulties in scale-up [35].

Here, for the first time, we present the concept of encapsulating ZSM-5 in MCM-41 particles using a one-pot, facile and scalable aerosolbased method. The aerosol-based (or spray pyrolysis) method is a wellknown technique for the rapid production of functional inorganic materials and the generation of hollow structures. The method was originally pioneered by Lu et al. for the synthesis of well-ordered mesoporous spheres of MCM-41 [36]. This is an example of the chemistry within the confined environment of aerosol droplet, where the use of MCM-41 precursors (e.g. tetraethoxysilane, TEOS) and the templating agent (cetyltrimethylammonium bromide, CTAB) are presented in the aerosol precursor solution and thus, in the droplets. As the droplets pass through a heated tube furnace, silica hydrolysis and condensation occur rapidly with templating to rapidly produce MCM-41. The method has been expanded in our laboratories for the synthesis of metal containing [37,38] and hollow silica particles where the control of templating can lead to novel morphologies [39,40]. The method is also easily scalable and can be adapted to continuous processing.

The novelty of our concept in this paper was to integrate ZSM-5 microcrystals into the precursor slurry where the ZSM-5 microcrystal size is significantly smaller than the orifice size of the aerosolizer (1 mm). As a result, the zeolite microcrystals are entrained in the aerosol droplet as shown schematically in Fig. 1a. As the droplets pass through the furnace zone, templated synthesis occurs with the evaporation of the solvent and the hydrolysis and condensation of MCM-41 around the ZMS-5 crystallites. Fig. 1a is a schematic of the translation of a droplet to a solid particle of MCM-41 containing dispersed ZSM-5 vicrocrystals. We should emphasize that this is not a core-shell struce in the strict definition of the term, but rather a composite

containing ZSM-5 microcrystal distributed in a spherical matrix of MCM-41. This is the first time that such a composite has been reported and tested for the CFP of biomass. The aerosol process is inherently amenable to scale up and continuous operation.

Our hypothesis was that the MCM-41 would act as a sacrificial layer for coke deposition, reducing the rate of ZSM-5 deactivation due to coke formation. The novel composites were prepared using the aerosol method with various ZSM-5 to MCM-41 ratios, were characterized and tested for CFP of miscanthus. Our main goal through this study was to prove that the ZSM-5 acid sites in the composites are fully accessible, and that the composites with high concentration of ZSM-5 result in: a) reduced rate of deactivation, and b) comparable (even improved) hydrocarbon yields to pure ZSM-5.

2. Experimental

2.1. Materials

Miscanthus \times giganteus was selected as biomass feedstock for pyrolysis, the proximate analysis, ultimate analysis and other properties of the biomass can be found in our previous study [41]. ZSM-5 (CBV 8014) was purchased from Zeolyst International, Inc. Pyridine (99 % purity), tetraethyl orthosilicate (TEOS, 98 %), hexadecyltrimethylammonium bromide (CTAB, 95 %) and hydrochloric acid (HCl, 37 %) were purchased from Sigma-Aldrich. Deionized (DI) water with a resistance of 18.2 M Ω was obtained from an Elga water purification system (Medica DV25).

2.2. Materials preparation

The composite ZSM-5 in MCM-41 catalysts were synthesized via a unique spray drying technique first reported by Lu et al. for the synthesis of mesoporous silica particles [36]Briefly, 1.5 g of cetyltrimethylammonium bromide (CTAB) was dissolved in 10 ml of ethanol under magnetic stirring. To achieve 50 wt.% ZSM-5 in the composite material, 0.58 g of ZSM-5 was added to the CTAB solution followed by ultrasonication in a bath sonicator (Cole-Parmer 8890) for 5 min to disperse the ZSM-5 crystals evenly in the solution. 4.5 ml of TEOS was added dropwise to the ZSM-5 suspension followed by 2 ml of 0.1 M HCl. This precursor suspension was allowed to stir for 10 min before transferring into the Nebulizer. The amount of ZSM-5 was adjusted to achieve the desired concentration of ZSM-5 in the composite (25%/ 50%/75%). More details on the spray drying method and a schematic diagram of the set up can be found in the Supplementary Information (Fig. S1). The catalyst materials were collected on a filter paper, transferred into an aluminum boat and calcined in air at 550 $^{\circ}\text{C}$ for 5 h at a heating rate of 5 °C/min to remove the organic template and obtain the porous material. MCM-41 particles were also synthesized as a control catalyst using the same methodology and quantities of reagents except for the addition of ZSM-5.

2.3. Materials characterization

The surface area and porosity of each material were determined by $N_2\,$ adsorption-desorption using a Micromeritics, ASAP 2010 Physisorption Analyzer. Prior to analysis, each sample was degassed for 12 h at 200 °C under vacuum. N_2 adsorption-desorption isotherms were then collected at 77 K. Surface areas were calculated based on Brunauer–Emmett–Teller (BET) method.

X-ray diffraction patterns were obtained using a Bruker D8 Advance powder diffractometer (CuK α radiation source). Electron microscopy was used to visualize the morphology of the synthesized catalysts. Scanning Electron Microscopy (SEM) was carried out using a Hitachi S-4800 field emission scanning electron microscope operated at 3 kV, while Transmission Electron Microscopy (TEM) was carried out on a FEI Tecnai G2 F30 twin transmission electron microscope operated at

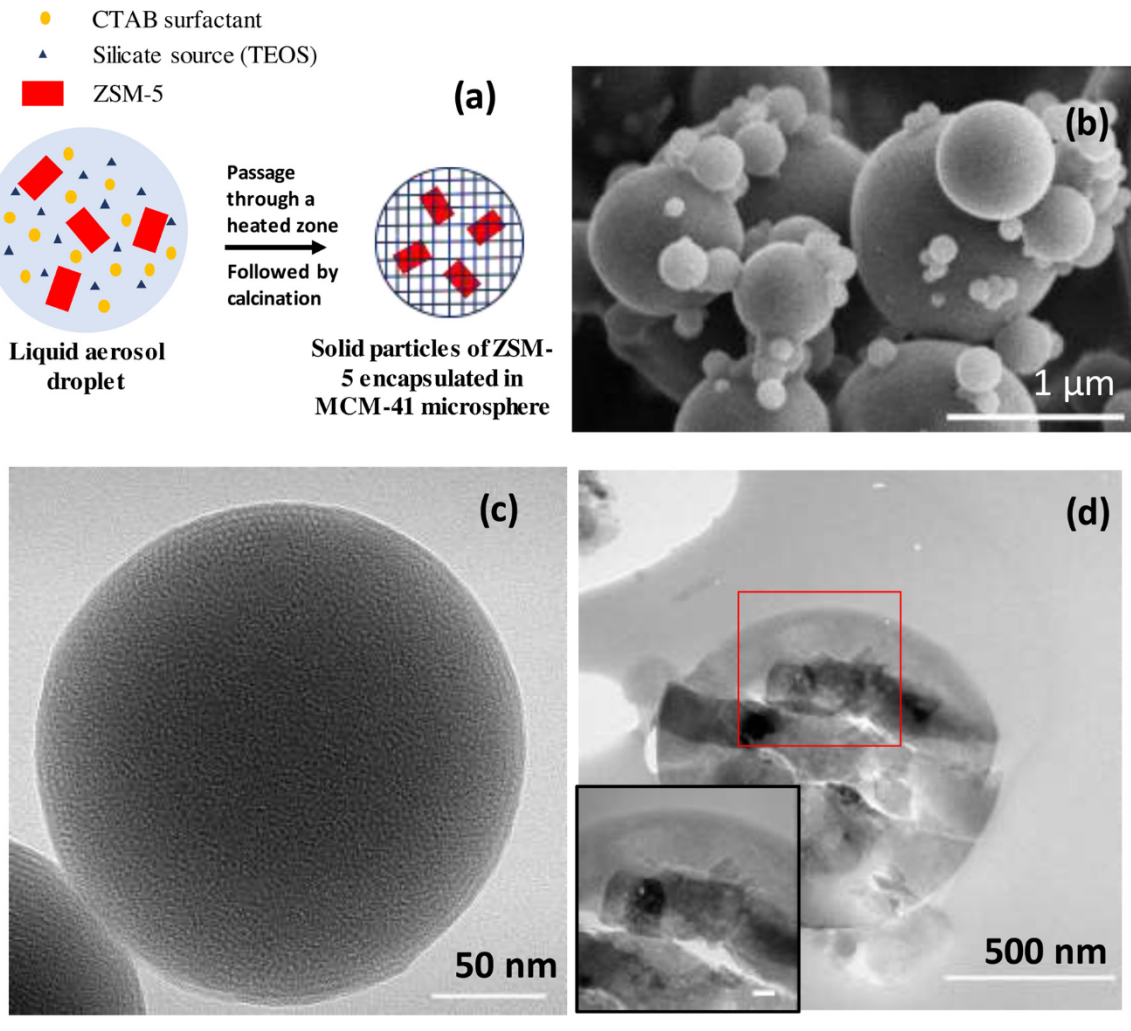


Fig. 1. (a) Schematic showing the concept of ZSM-5 encapsulation in mesoporous MCM-41 microsphere, (b) SEM showing polydispersity and spherical morphologies of the particles, (c) TEM of a single particle and (d) cut-section TEM images of composite MCM-41/50%ZSM-5. ZSM-5 microcrystals are reflected in the small particles with sharp edges.

300 kV.

Pyridine adsorption was conducted to measure the acidity of the catalysts using Diffuse Reflectance Infrared Fourier Transform Spectroscopy (DRIFTS). Spectra were collected on a Thermo Nicolet 6700 FTIR spectrometer coupled with a temperature controlled Harrick Praying Mantis DRIFTS accessory. Background was obtained at 120 $^{\rm o}$ C before any sample loading. Prior to analysis, samples were first calcined *in-situ* for 1 h at 550 $^{\rm o}$ C under N_2 atmosphere. The spectra of materials before adsorption were recorded at 120 $^{\rm o}$ C. Afterwards, pyridine adsorption was carried out at 120 $^{\rm o}$ C. After adsorption, the chamber was slowly heated to 250 $^{\rm o}$ C under vacuum to remove physisorbed pyridine. Then the samples were cooled to 120 $^{\rm o}$ C and spectra were collected at that temperature. The final spectra displayed in this paper were formed by subtracting the spectra obtained before and after adsorption.

2.4. In-situ Py-GC experiments

CFP experiments were performed using a Py-GC/MS system (CDS Analytical Inc. 5200HP) in either *in-situ* or *ex-situ* mode [42]. A scheme of the apparatus is provided in supplementary information (SI). For *in-situ* experiments, catalysts were first mixed with biomass at a specific catalyst to biomass (C/B) ratio (here 5:1). $5\pm0.1\,\mathrm{mg}$ of the mixture (or pure biomass) was plugged into a quartz tube microreactor and andwiched by two pieces of quartz wool. During pyrolysis, the intere was maintained at 300 °C to prevent any condensation of volatiles

and Ar was used as carrier gas. The coil around the microreactor was rapidly heated to 600 °C and maintained for 20 s to pyrolyze biomass. The generated condensable vapors were captured by a cold trap and non-condensable gases were sent to an online mass spectroscopy system (MS, Agilent 5975C). The MS was calibrated for H2, CO, CO2, CH4 and Ar prior to experiments. After pyrolysis was completed, the condensed liquid products were desorbed from the trap and transferred through a transfer line, which was heated to 300 °C, to a gas chromatography-mass spectroscopy system (GC-MS, Agilent 6890 GC with 5973 N MS) for analysis. The GC-MS was calibrated externally by injecting prepared standards through the pyrolyzer. Only the compounds with a qualifier larger than 75 were quantified for further analysis. Solid product yields were acquired via the oxidation of the residue in the microreactor at 950 °C. The generated CO2 was measured by MS and used to calculate solid yields. The yields of products in this study were calculated based on carbon balance.

Thermogravimetric analysis (TGA) was performed to analyze the composition of solid mixture after *in-situ* CFP. TGA was conducted using a TGA Q500 (TA instruments). The solids were heated at a heating rate of $10\,^{\circ}\text{C}$ from $50\,^{\circ}\text{C}$ to $800\,^{\circ}\text{C}$ under air flow. The mass change during programmed oxidation was recorded and its derivative was plotted.

All the results on the yields of products are based on carbon balance.

2.5. Ex-situ Py-GC experiments

Ex-situ experiments were carried out using the same instruments and analysis methods that were used for in-situ experiments. For ex-situ configuration, $2\pm0.1\,\mathrm{mg}$ of biomass was placed in the quartz tube microreactor and $10\pm0.1\,\mathrm{mg}$ of catalysts were packed in a tandem fixed-bed reactor, thus, the catalyst to biomass ratio was maintained at 5:1. The temperature of fixed-bed reactor was kept at 600 °C during pyrolysis. The pyrolysis method was the same as for in-situ experiments. To evaluate the longevity of catalyst activity, three ex-situ experiments were performed in series for each catalyst. The spent catalysts were either regenerated or not regenerated to study the accumulation of coke over consecutive experiments. The regeneration of catalyst was carried out by changing the fixed-bed temperature to 800 °C and switching the carrier gas to oxygen. The generated CO₂ were detected by MS and used to calculate the yield of coke. All the results on the yields of products are based on carbon balance.

3. Results and discussion

3.1. Characterization results

Fig. 1a is a schematic of the aerosol process for integrating ZSM-5 microcrystals in an MCM-41 particle, while Fig. 1b-d show electron micrographs of the resulting particles. The SEM image in Fig. 1b shows a wide distribution of particle sizes and the polydispersity is an inherent feature of the aerosol process. However, there is an additional aspect here as the larger particles typically contain the zeolite while the small particles reflect droplets that do not contain ZSM-5 when ejected through the nozzle and that result exclusively in MCM-14. Fig. 1c shows TEMs of an assembly of particles and all particles reflect a spherical morphology and are porous reflecting the mesopore structure of MCM-41 that can be seen through TEM at the periphery of the particle. We note that ZSM-5 is not visible to the direct TEM image of Fig. 1c but cutsections of the particles clearly reveal the sharper edges of the zeolite microcrystals (Fig. 1d). The details of the BET surface areas and x-ray diffraction patters of all composites, as well as the SEM and TEM images are presented in the SI section and a second manuscript has been written to describe all details of catalyst preparation and to characterize reaction and diffusion in these systems using the model reaction of the liquid phase amination of nitrophenol. The present paper describes the details of such composite catalyst pellets as directed to the CFP of

Pyridine adsorption of catalysts was performed using a DRIFT cell. The final spectra shown in Fig. 2 was derived by subtracting the spectra of materials before and after adsorption. Peaks at around 1550 and

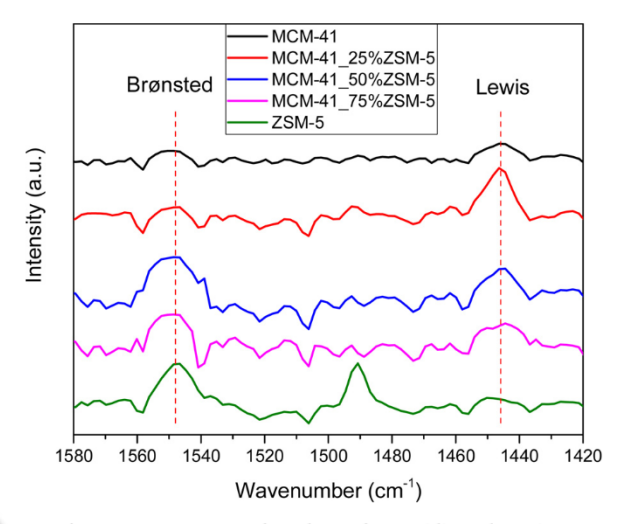


Fig. 2. DRIFT spectra of catalysts after pyridine adsorption.

Table 1
The concentrations of Brønsted and Lewis acid sites and their ratio of each catalyst.

Material	Brønsted acid sites $(\mu mol g^{-1})$	Lewis acid sites $(\mu \text{mol g}^{-1})$	B.A./L.A Ratio
MCM-41	1.41	1.12	1.26
MCM-41_25%ZSM-5	1.84	2.49	0.74
MCM-41_50%ZSM-5	3.26	2.71	1.20
MCM-41_75%ZSM-5	3.78	2.38	1.59
ZSM-5	4.98	0.86	5.77

1450 cm⁻¹ correspond to Brønsted acid sites and Lewis acid sites, respectively. The concentration of Brønsted and Lewis acid sites, as well as their ratios are presented in Table 1. The extinction coefficients used for the calculation of Brønsted and Lewis acid site concentrations were 1.67 cm/µmol and 2.22 cm/µmol, respectively [43]. As expected, MCM-41 showed very low concentration of Brønsted and Lewis acid sites, since it is a solely siliceous material, while ZSM-5 showed high Brønsted acidity. Increasing the ZSM-5 content in the composite, the concentration of Brønsted acid sites also increased. However, the concentrations of Lewis acid sites on those composites were higher than both ZSM-5 and MCM-41 and did not show a clear trend with the ZSM-5 content in the composite. It is difficult to explain the presence of Lewis acidity in the composites. We hypothesize that it might be attributed to the combustion of carbonaceous materials (here CTAB) during calcination [44].

3.2. In-situ Py-GC experiments

In-situ CFP of miscanthus × giganteus experiments were performed either without any catalyst or with catalyst in a C/B of 5:1. The C/B ratio of 5:1 is typical and comparable with other similar studies in literature, as well as with our previous studies [8,42,45,46]. The catalysts used were the composites with various concentrations of ZSM-5: from 0 (pure MCM-41) to 100 % (pure ZSM-5). Fig. 3a-c show the overall product yields, permanent gas yields and liquid product yields distribution, respectively. The overall product yields are based on carbon balance (water was not included) and the results show similar trends and are in good agreement with our previous studies as well as other studies in literature [8,30,42,45]. A detailed comparison of CFP in PyGC with a spouted bed lab scale reactor can also be found is our previous study [42]. As shown in Fig. 3a, pyrolysis experiments without any catalyst resulted in a significant yield of liquid products and the least yield of gas and solid products, compared to any other CFP experiments. As shown in Fig. 3c, in the absence of catalyst, the liquid product was composed of oxygenates only. By introducing pure MCM-41, a substantial increase on the solid yields was observed, accompanied with an increase of CO and CO2 yields and a simultaneous drop of oxygenates yield in the liquid. The decline of liquid yield in the presence of catalyst was also observed by other researchers [9,47-49]. Chen et al. [47] observed that the pyrolysis of cotton stalk without catalyst produced the highest amount of bio-oil, while in the presence of any catalyst, the liquid yield dropped. The decline was most significant using MCM-41. In our study, we hypothesize that the vapors (mainly oxygenates) generated from the pyrolysis of miscanthus diffused into the MCM-41 particles and they were condensed and transformed into coke and char, thus increasing the solid yield. Some decarbonylation and decarboxylation reactions took place according to the increased yield of CO and CO2, while almost no hydrocarbons were produced, indicating the formation of coke. When 25 % of ZSM-5 was introduced in the composite, the overall carbon yield distribution did not change significantly. However, some hydrocarbons started to appear in the liquid product. It seems that the acid sites of ZSM-5 were accessible to biomass pyrolysis vapors, where both cracking and deoxygenation reactions were enhanced. As the composition of ZSM-5

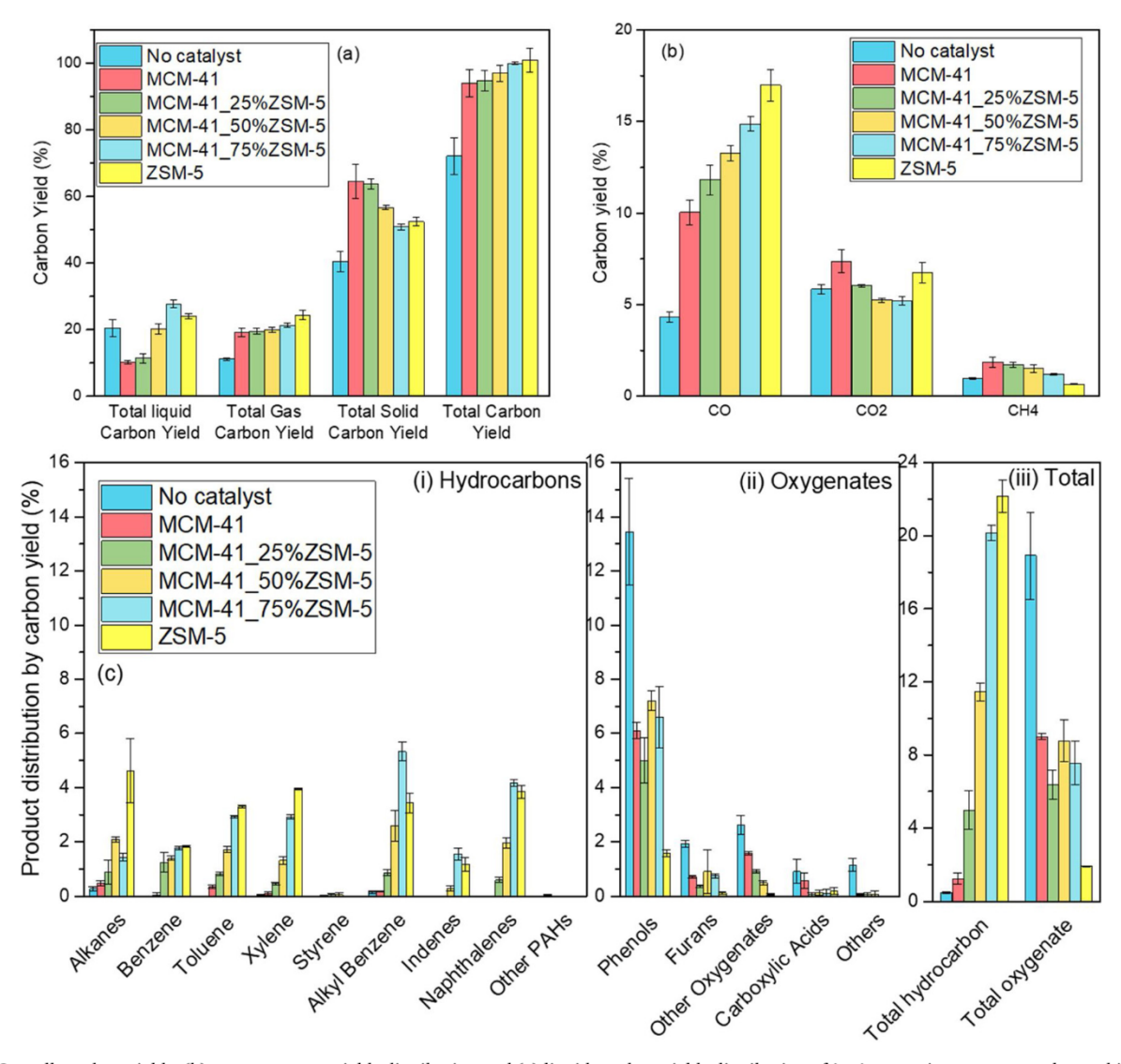


Fig. 3. (a) Overall product yields, (b) permanent gas yields distribution and (c) liquid product yields distribution of *in-situ* experiments at a catalyst to biomass ratio of 5:1.

in the composite became higher, the acid catalyzed reactions became more significant and the selectivity of hydrocarbons in the liquid increased drastically.

The yield of benzene, toluene and xylene (BTX) ascended gradually by increasing the ZSM-5 content from 25 % to 100 %. Although 100 % ZSM-5 showed a much higher yield of alkanes compared to other materials, the composite with 75 % of ZSM-5 showed slightly higher yield of alkyl benzene, indenes and naphthalenes, than pure ZSM-5. In terms of total hydrocarbon yield, the composite with 75 % of ZSM-5 showed very close performance to pure ZSM-5. However, the composites showed higher oxygenates yields than pure ZSM-5 (100 %). Probably in the absence of the MCM-41 layer, more active sites on the outer surface of ZSM-5 were available and therefore, enhanced the deoxygenation reactions.

For comparison reasons, *in-situ* experiments using pure ZSM-5 with different ZMS-5 to biomass ratios were conducted and the results are presented in Fig. 4. The C/B ratio varied from 1.25 to 5, to match the ZSM-5 to biomass ratio using the composites (*e.g.* the experiment using pure ZSM-5 at C/B ratio of 1.25 was performed for comparison with the experiment using the composite with 25 % of ZSM-5 at C/B ratio of 5). Using pure ZSM-5, the total liquid yield and gas yield increased slightly as the ZSM-5 to biomass ratio increased, while solid yield fluctuated tween 45 % and 55 %. In liquid products, nearly all hydrocarbon

yields increased as ZSM-5 to biomass ratio increased, while the yields of all oxygenates dropped, which was consistent with our previous study [42]. Compared to the experimental data using the composites with the same amount of ZSM-5, it appears that at ZSM-5 to biomass ratio of 1.25:1, the pure ZSM-5 showed higher total hydrocarbon and oxygenate yield than the corresponding composite. This might be attributed to the condensation of pyrolysis vapors on the MCM-41 surface, before they reach the active sites of ZSM-5. At ZSM-5 to biomass ratio of 2.5:1, the difference of total hydrocarbon and oxygenate yields between the pure ZSM-5 and the corresponding composite became smaller, indicating that more pyrolysis vapors were able to contact the ZSM-5 and diffuse out of the composite. At ZSM-5 to biomass ratio of 3.75:1, the composite and the pure ZSM-5 showed approximately the same performance. That is an evidence of full accessibility of ZSM-5 in the composite.

In our earlier studies we have proved that TGA is a powerful tool to understand the origin of carbon in the solid residue derived from CFP. We have clearly demonstrated that char is a carbonaceous deposit that appears at around 400 °C, while coke on catalyst appears at around 700 °C. When catalyst and biomass are blended (*in situ* CFP), there is a displacement of both peaks. The area under the peaks is relevant to the amount of char and coke generated by the pyrolysis. More information on the origin of coke and char can be found in our previous studies

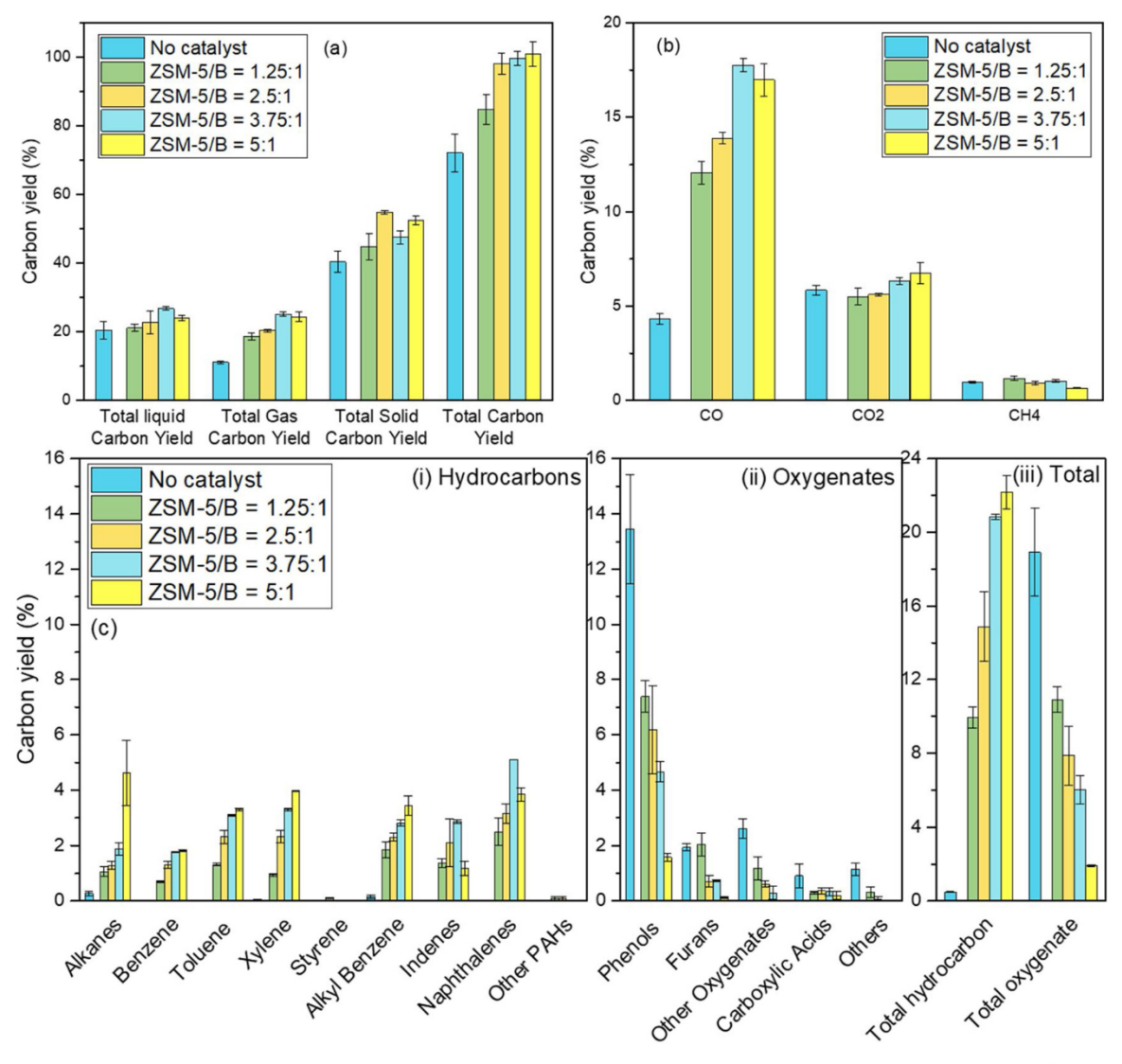


Fig. 4. (a) Overall product yields, (b) permanent gas yields distribution and (c) liquid product yields distribution of *in-situ* experiments at different pure ZSM-5 to biomass ratios.

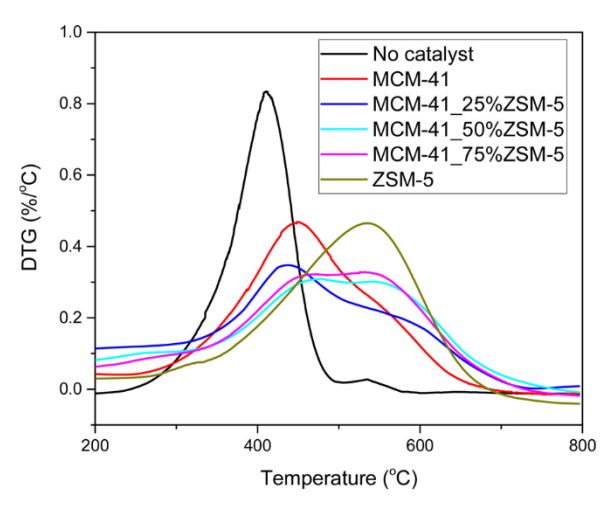


Fig. 5. DTG analysis of solid residues after in-situ pyrolysis experiments.

[6,42]. TGA was conducted in the present study to identify the state of solid residues after the *in-situ* CFP using the composites. The first devative of TG curve (DTG) is shown in Fig. 5. When pyrolysis was

performed in the absence of catalyst, there was only one DTG peak at approximately 400 °C, which was assigned to biochar. Using pure MCM-41, the peak was shifted to approximately 450 °C. This shift was probably attributed to the formation of oxygen-rich coke on MCM-41, which was likely generated by the reformation of biochar and the condensation of the pyrolysis vapors. Preliminary deoxygenation reactions might have taken place during the process, which can be confirmed by the increase of CO yield using pure MCM-41 as catalyst. On the other hand, the solid residue derived from pyrolysis using pure ZSM-5 showed a peak at approximately 550 °C, indicating coke formation with low oxygen content.

Summarizing, two types of products were identified *via* TGA analysis of the solid residues obtained by *in-situ* pyrolysis: a) carbons derived by MCM-41 oxidized at 450 °C and b) carbons derived by ZSM-5 oxidized at 550 °C. With this difference in mind, the solid products produced by composites can be analyzed. The solid produced by the composite with 25 % of ZSM-5 showed a peak at 450 °C and a shoulder at 550 °C, indicating that the majority of the solid was composed of the coke formed by MCM-41. As the content of ZSM-5 became higher, the peak area of coke attributed to MCM-41 became lower, while the contribution of the coke attributed to ZSM-5 became more significant. Therefore, we hypothesize that the MCM-41 in the composites can act as a sacrificial layer for the deposition of coke in ZSM-5; this layer

might consequently allow ZSM-5 to maintain its activity longer.

The reaction mechanism of biomass CFP using ZSM-5 has been discussed by various studies [50-53]. In summary, the three initial components of biomass (cellulose, hemi-cellulose and lignin) break down in a thermal reaction to form primary pyrolysis products, namely soluble sugars. The latter further thermally decompose to form carboxylic acids. These carboxylic acids may then undergo a series of dehydration, decarboxylation, fragmentation, condensation and cyclization reactions to form functionalized furans. Lignin may also break down to form guaiacols, which further react to form phenols. In the presence of catalyst (ZSM-5) the acids, furans and phenols undergo decarboxylation and decarbonylation reactions to form gases (CO and CO₂) and aromatics. In light of the aforementioned generic reaction mechanis, our in-situ experiments presented in this study revealed that increasing the ZSM-5 content in the composite, significantly increases the total hydrocarbon yield, suggesting that the ZSM-5 is fully accessible and the decarboxylation and decarbonylation reactions are promoted. Pure MCM-41 does not promote the aforementioned acid catalyzed reactions, leading to bio-oils which contain mainly oxygenates. Pure ZSM-5 showed higher hydrocarbon yields, than the corresponding composites at the same ZSM-5/biomass ratio. However, when the ZSM-5 to biomass ratio became high, that difference became small. From the total hydrocarbon yield and CO yield, it can be concluded that the active sites of ZSM-5 in the composite were accessible, but the activity was slightly lower than pure ZSM-5, probably because of the coverage of the acid sites on the outer surface of ZSM-5 by the MCM-41 shell. Fig. 6 is a simplified schematic which summarizes the mechanism for CFP of biomass by the composites with the different ZSM-5 content.

3.3. Ex-situ Py-GC experiments

Ex-situ experiments were performed to study the coke formation and the regeneration of the catalysts. The catalyst to biomass ratio was kept at 5:1, for each catalyst. Three consecutive CFP experiments were performed without regeneration in between. Thus, the solid carbon yield, i.e. the coke deposited after each one of the three experiments, was not measured. Fig. 7 shows the total hydrocarbon yields and total oxygenate yields of three consecutive experiments for each catalyst. Detailed distribution of each compound in the liquid phase and gas products can be found in the SI.

In the first experiment of each composite, as the content of ZSM-5 increased in the composite, more hydrocarbons were produced (Fig. 7a). The composite with 75 % of ZSM-5 showed total hydrocarbon yield approximately the same as the pure ZSM-5, suggesting a high activity of MCM-41_75%ZSM-5 composite. The oxygenate yield reached a maximum at 25 % of ZSM-5 and then decreased. The high total oxygenates yield by MCM-41_25%ZSM-5 was a result of high production of phenols and furans.

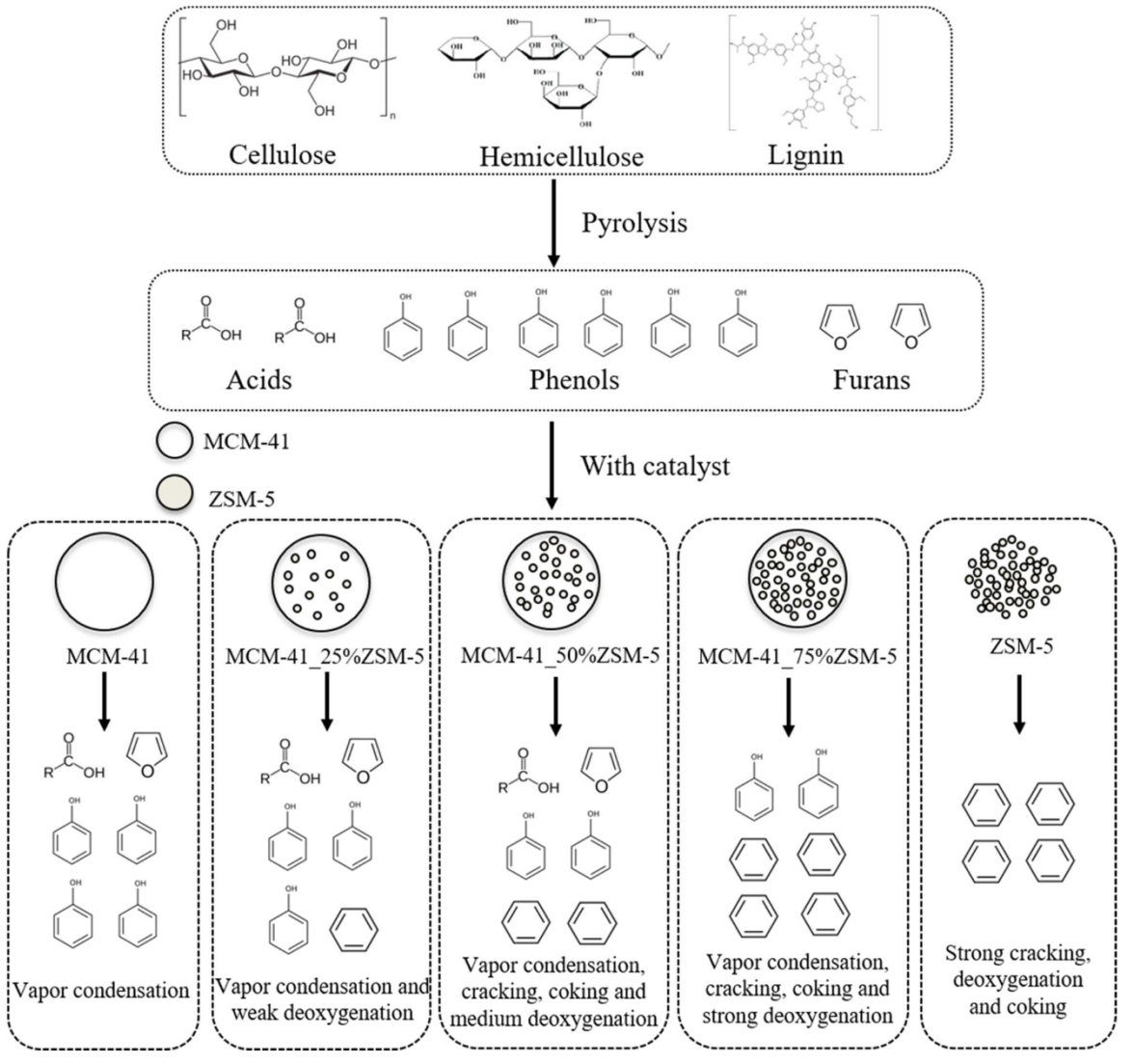


Fig. 6. Simplified schematic of the CFP of miscanthus using the MCM-41/ZSM-5 composites.

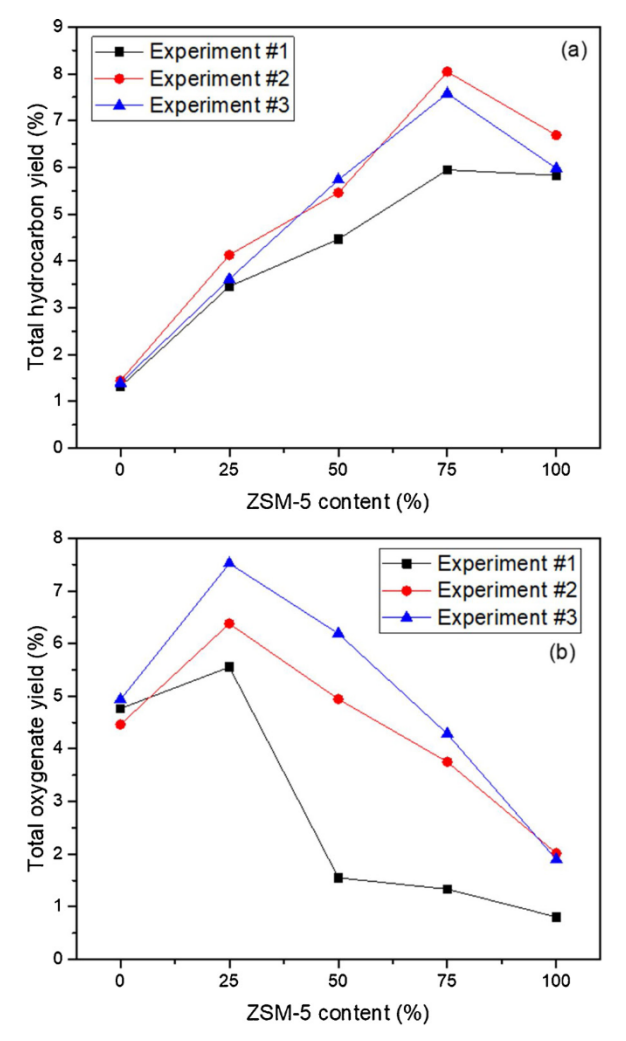


Fig. 7. (a) Total hydrocarbon yield and (b) total oxygenate yield of *ex-situ* experiments at a catalyst to biomass ratio of 5 to 1 by the catalysts/composites with various ZSM-5 content.

In their second experiment, all of catalysts showed higher hydrocarbon and oxygenate yield. This increase of the liquid yield might be attributed to the decrease of the solid yield. The most active acid sites had been covered by coke during the first experiment, so less coke would form during the second or third experiment. Similar trend has been observed by Xu et al. [28]. The total hydrocarbon yield by the composite with 75 % of ZSM-5 increased substantially in the second experiment, while pure ZSM-5 showed only a small increase. The increase of total hydrocarbon yields by MCM-41_75%ZSM-5 composite was mainly attributed to large hydrocarbon compounds, such as indenes and naphthalenes. As suggested by other researchers, indenes and naphthalenes are important precursors of coke [54]. The increase in indenes and naphthalenes yields suggested that less large hydrocarbon molecules were further converted to coke.

As for the third experiment, the total hydrocarbon yield was slightly lower than the second experiment for most of catalysts, while the yield of total oxygenate yield kept increasing. The decrease of hydrocarbon yield and the increase of oxygenate yield might be attributed to the deactivation of catalysts.

Comparing the liquid and gas yields derived from the first experiment using the 75 % ZSM-5 composite and the pure ZSM-5, it appears that they had very similar product yield and distribution, except of the CO₂ yield. Pure ZSM-5 showed a higher CO₂ yield, indicating that it promoted decarboxylation reactions. However, the stronger decarboxylation reactions by the pure ZSM-5 did not result in higher

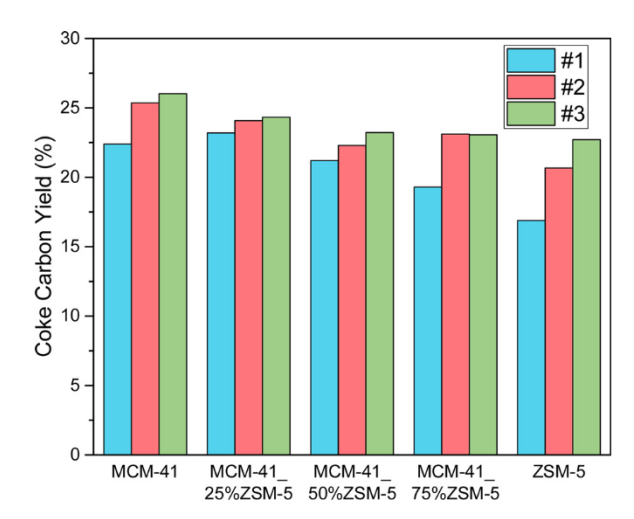


Fig. 8. Coke carbon yields of *ex-situ* experiments with regeneration at a catalyst to biomass ratio of 5 to 1.

hydrocarbon yield, compared to MCM-41_75%ZSM-5. Hence, we hypothesize that in the case of pure ZSM-5, the decarboxylation reactions were more likely ascribed to coke condensation (where coke lost oxygen in the form of CO_2) than deoxygenation of liquid products; thus, more CO_2 was generated without affecting the yield of hydrocarbons. Therefore, the composite with 75 % of ZSM-5 can maintain a high activity and limit the undesired coke condensation reactions at the same time. This conclusion is consistent with our hypothesis that MCM-41 layer can act as a sacrificial layer for coke deposition.

Coke deposition on catalyst during *ex-situ* CFP is a crucial concern. Because in the aforementioned consecutive experiments, coke was not measured, additional experiments followed by regeneration were performed to measure the yield of coke for each catalyst. The experimental conditions were kept the same as in the consecutive experiments, and the catalysts were regenerated at 800 °C after each experiment using pure O_2 . The comparison of coke yields for all of catalysts are shown in Fig. 8. MCM-41 showed relatively higher coke yield than ZSM-5. With increasing the ZSM-5 content from 25 % to 100 %, the coke yield declined gradually in the first run-regeneration cycle. At the second and third run-regeneration cycles, the coke yield increased gradually by all of catalysts, as a result of irreversible deactivation. However, it appears that the deactivation was less severe for the composites, than the pure ZSM-5 catalyst. Therefore, with the protection of MCM-41, the composites can prolong the lifetime of active ZSM-5 inside the particle.

The ex-situ experiments highlighted the advantages of MCM-41_ZSM-5 composites. In the first run of a series of ex-situ experiments, as the content of ZSM-5 increased in the composite, more hydrocarbons were produced. The composite with 75 % of ZSM-5 resulted in approximately the same total hydrocarbon yield with the pure ZSM-5, suggesting a high activity of the former. In the second run, all of catalysts showed higher hydrocarbon and oxygenate yields, compared to the first run. This increase of the liquid yield might be attributed to the decrease of the solid yield. The total hydrocarbon yield by the composite with 75 % of ZSM-5 increased substantially in the second run, while pure ZSM-5 showed only a small increase. The increase of total hydrocarbon yields by MCM-41_75%ZSM-5 composite was mainly attributed to heavy hydrocarbon molecules, such as indenes and naphthalenes. In the third run, the total hydrocarbon yield was slightly lower than the second run for most of catalysts, while the yield of total oxygenates yield kept increasing, indicating the deactivation of catalysts. Pure ZSM-5 showed a higher CO2 yield, indicating that it promoted decarboxylation reactions, while the hydrocarbon production was not enhanced. This suggests that the decarboxylation reactions were likely ascribed to coke condensation (where coke lost oxygen in the form of CO₂), rather than deoxygenation of liquid products. With increasing the ZSM-5 content from 25 % to 100 %, the coke yield declined gradually in the first run-regeneration cycle. The coke yield increased faster for pure ZSM-5 than the composites as more run-regeneration cycles were performed.

4. Conclusions

Novel MCM-41/ZSM-5 composites with ZSM-5 crystals encapsulated in MCM-41 particles were successfully prepared by a one-step aerosol method. The concentration of ZSM-5 in the composites was varied from 0 % to 75 %. The successful encapsulation of ZSM-5 was evident by various characterization techniques. The composites were tested for the *in-situ* and *ex-situ* CFP of miscanthus. The *in-situ* experiments revealed that increasing the ZSM-5 content in the composite, significantly increases the total hydrocarbon yield, suggesting that the ZSM-5 in the composites is fully accessible. The composite with 75 % of ZSM-5 achieved a comparable hydrocarbon yield to pure ZSM-5, while the MCM-41 shell acted as a sacrificial layer for coke deposition and protected the ZSM-5 from severe coking. TGA results revealed that coke was formed on MCM-41 shell and reduced the amount of coke on ZSM-5.

Sequential *ex-situ* experiments showed that MCM-41_75%ZSM-5 was excellent on maintaining hydrocarbon yields over three consecutive runs. The run-regeneration experiments showed that MCM-41/ZSM-5 composites can reduce the rate of coke formation, compared to pure ZSM-5. These results suggest that the MCM-41-ZSM-5 composite with high ZSM-5 content (75 %) is a promising material for the CFP of biomass, in terms of its good catalytic performance and more importantly, tolerance to deactivation.

CRediT authorship contribution statement

Lei Yu: Methodology, Investigation, Validation, Writing - original draft. Azeem Farinmade: Methodology, Investigation, Resources. Oluwole Ajumobi: Methodology, Investigation, Resources. Yang Su: Resources. Vijay T. John: Conceptualization, Writing - review & editing, Supervision, Funding acquisition. Julia A. Valla: Conceptualization, Writing - review & editing, Supervision, Funding acquisition.

Declaration of Competing Interest

The authors declare that they have no known competing financial interests or personal relationships that could have appeared to influence the work reported in this paper.

Acknowledgement

We gratefully acknowledge funding from National Science Foundation (NSF grant number: CMMI 1826146).

Appendix A. Supplementary data

Supplementary material related to this article can be found, in the online version, at doi:https://doi.org/10.1016/j.apcata.2020.117727.

References

- [1] X. Chen, Q. Che, S. Li, Z. Liu, H. Yang, Y. Chen, X. Wang, J. Shao, H. Chen, FUEL Process. Technol. 196 (2019).
- [2] Y.M. Kim, J. Jae, B.S. Kim, Y. Hong, S.C. Jung, Y.K. Park, Energy Convers. Manage. 149 (2017) 966–973.
- [3] D.P. Gamliel, L. Wilcox, J.A. Valla, Energy Fuels 31 (2017) 679–687.
- [4] D.P. Gamliel, G.M. Bollas, J.A. Valla, Fuel 216 (2018) 160-170.
- [5] Y. Chi, J. Xue, J. Zhuo, D. Zhang, M. Liu, Q. Yao, Sci. Total Environ. 633 (2018) 1105–1113.

- [6] S. Du, J.A. Valla, G.M. Bollas, Green Chem. 15 (2013) 3214-3229.
- [7] M. Yang, J. Shao, H. Yang, K. Zeng, Z. Wu, Y. Chen, X. Bai, H. Chen, Bioresour. Technol. 273 (2019) 77–85.
- [8] K. Soongprasit, V. Sricharoenchaikul, D. Atong, J. Anal. Appl. Pyrolysis 139 (2019) 239–249.
- [9] Z. Ma, E. Troussard, J.A. Van Bokhoven, Appl. Catal. A Gen. 423–424 (2012) 130–136.
- [10] K. Iisa, R.J. French, K.A. Orton, S. Budhi, C. Mukarakate, A.R. Stanton, M.M. Yung, M.R. Nimlos, Top. Catal. 59 (2016) 94–108.
- [11] S. Kelkar, C.M. Saffron, K. Andreassi, Z. Li, A. Murkute, D.J. Miller, T.J. Pinnavaia, R.M. Kriegel, Appl. Catal. B Environ. 174–175 (2015) 85–95.
- [12] D.P. Gamliel, G.M. Bollas, J.A. Valla, Energy Technol. 5 (2017) 172-182.
- [13] T. Mochizuki, D. Atong, S.Y. Chen, M. Toba, Y. Yoshimura, Catal. Commun. 36 (2013) 1–4.
- [14] V.B.F. Custodis, S.A. Karakoulia, K.S. Triantafyllidis, J.A. Van Bokhoven, ChemSusChem 9 (2016) 1134–1145.
- [15] S.D. Stefanidis, S.A. Karakoulia, K.G. Kalogiannis, E.F. Iliopoulou, A. Delimitis, H. Yiannoulakis, T. Zampetakis, A.A. Lappas, K.S. Triantafyllidis, Appl. Catal. B Environ. 196 (2016) 155–173.
- [16] Y.Y. Chong, S. Thangalazhy-Gopakumar, H.K. Ng, S. Gan, L.Y. Lee, P.B. Ganesan, Clean Technol. Environ. Policy 21 (2019) 1629–1643.
- [17] X. Xue, Z. Pan, C. Zhang, D. Wang, Y. Xie, R. Zhang, Environ. Prog. Sustain. Energy 38 (2019) 1–7.
- [18] S. Wan, T. Pham, S. Zhang, L. Lobban, D. Resasco, R. Mallinson, AIChE J. 61 (2015) 857–866.
- [19] J. Gou, Z. Wang, C. Li, X. Qi, V. Vattipalli, Y.T. Cheng, G. Huber, W.C. Conner, P.J. Dauenhauer, T.J. Mountziaris, W. Fan, Green Chem. 19 (2017) 3549–3557.
- [20] A. Kumar, A. Kumar, J. Kumar, T. Bhaskar, Bioresour. Technol. 291 (2019) 121822.
- [21] S. Shao, H. Zhang, R. Xiao, X. Li, Y. Cai, J. Anal. Appl. Pyrolysis 127 (2017) 258–268.
- [22] H. Zhang, S. Shao, R. Xiao, D. Shen, J. Zeng, Energy Fuels 28 (2014) 52-57.
- [23] S. Du, D.P. Gamliel, M.V. Giotto, J.A. Valla, G.M. Bollas, Appl. Catal. A Gen. 513 (2016) 67–81.
- [24] A.R. Stanton, K. Iisa, C. Mukarakate, M.R. Nimlos, ACS Sustain. Chem. Eng. 6 (2018) 10030–10038.
- [25] X. Xue, Y. Liu, L. Wu, X. Pan, J. Liang, Y. Sun, Bioresour. Technol. 289 (2019) 121691.
- [26] T.C. Hoff, M.J. Holmes, J. Proano-Aviles, L. Emdadi, D. Liu, R.C. Brown, J.P. Tessonnier, ACS Sustain. Chem. Eng. 5 (2017) 8766–8776.
- [27] H. Yang, R. Coolman, P. Karanjkar, H. Wang, P. Dornath, H. Chen, W. Fan, W.C. Conner, T.J. Mountziaris, G. Huber, Green Chem. 19 (2017) 286–297.
- [28] M. Xu, C. Mukarakate, K. Iisa, S. Budhi, M. Menart, M. Davidson, D.J. Robichaud, M.R. Nimlos, B.G. Trewyn, R.M. Richards, ACS Sustain. Chem. Eng. 5 (2017) 5477–5484.
- [29] D.P. Gamliel, H.J. Cho, W. Fan, J.A. Valla, Appl. Catal. A Gen. 522 (2016) 109-119.
- [30] C. Hu, H. Zhang, R. Xiao, J. Anal. Appl. Pyrolysis 136 (2018) 27–34.
- [31] Z. Li, Z. Zhong, B. Zhang, J. Gu, K. Shi, Energy Technol. 6 (2018) 728–736.
- [32] B. Zhang, J. Zhang, Z. Zhong, Y. Zhang, M. Song, X. Wang, K. Ding, R. Ruan, J. Anal. Appl. Pyrolysis 130 (2018) 249–255.
- [33] R. Zou, Y. Wang, L. Jiang, Z. Yu, Y. Zhao, Q. Wu, L. Dai, L. Ke, Y. Liu, R. Ruan, Bioresour. Technol. 289 (2019) 121609.
- [34] M. Li, Y. Hu, Y. Fang, T. Tan, Catal. Today 339 (2019) 312–320.
- [35] K. Li, J. Valla, J. Garcia-Martinez, ChemCatChem 6 (2014) 46–66.
- [36] Y. Lu, H. Fan, A. Stump, T.L. Ward, T. Rieker, C.J. Brinker, Nature 398 (1999) 223–226.
- [37] Y. Wang, B. Sunkara, J. Zhan, J. He, L. Miao, G.L. McPherson, V.T. John, L. Spinu, Langmuir 28 (2012) 13783–13787.
- [38] T. Zheng, J. Pang, G. Tan, J. He, G.L. McPherson, Y. Lu, V.T. John, J. Zhan, Langmuir 23 (2007) 5143–5147.
- [39] Y. Su, Y. Wang, O. Owoseni, Y. Zhang, D.P. Gamliel, J.A. Valla, G.L. McPherson, V.T. John, ACS Appl. Mater. Interfaces 10 (2018) 13542–13551.
- [40] Y. Su, O.F. Ojo, I.K.M. Tsengam, J. He, G.L. McPherson, V.T. John, J.A. Valla, Langmuir 34 (2018) 14608–14616.
- [41] S. Du, Y. Sun, D.P. Gamliel, J.A. Valla, G.M. Bollas, Bioresour. Technol. 169 (2014) 188–197.
- [42] D.P. Gamliel, S. Du, G.M. Bollas, J.A. Valla, Bioresour. Technol. 191 (2015) 187–196.
- [43] C.A. Emeis, J. Catal. 141 (1993) 347-354.
- [44] G.L. Woolery, G.H. Kuehl, Zeolites 19 (1997) 288–296.
- [45] Q. Lu, Z.X. Wang, H.Q. Guo, K. Li, Z.X. Zhang, M.S. Cui, Y.P. Yang, Fuel 243 (2019) 88–96.
- [46] K.G. Kalogiannis, S.D. Stefanidis, S.A. Karakoulia, K.S. Triantafyllidis, H. Yiannoulakis, C. Michailof, A.A. Lappas, Appl. Catal. B Environ. 238 (2018) 346–357.
- [47] X. Chen, Y. Chen, H. Yang, X. Wang, Q. Che, W. Chen, H. Chen, Bioresour. Technol. 273 (2019) 153–158.
- [48] J. Fermoso, H. Hernando, P. Jana, I. Moreno, J. Přech, C. Ochoa-Hernández, P. Pizarro, J.M. Coronado, J. Čejka, D.P. Serrano, Catal. Today 277 (2016) 171–181
- [49] J. Wang, Z. Zhong, Z. Song, K. Ding, A. Deng, Energy Convers. Manage. 123 (2016) 29–34.
- [50] Y. Berro, S. Gueddida, S. Lebègue, A. Pasc, N. Canilho, M. Kassir, F.E.H. Hassan, M. Badawi, Appl. Surf. Sci. 494 (2019) 721–730.
- M. Badawi, Appl. Surf. Sci. 494 (2019) 721–730.
 [51] M.S. Mettler, S.H. Mushrif, A.D. Paulsen, A.D. Javadekar, D.G. Vlachos, P.J. Dauenhauer, Energy Environ. Sci. 5 (2012) 5414–5424.
- [52] Y.T. Cheng, G.W. Huber, Green Chem. 14 (2012) 3114-3125.
- [53] R. Vinu, L.J. Broadbelt, Energy Environ. Sci. 5 (2012) 9808–9826.
- [54] H. Zhang, S. Shao, M. Luo, R. Xiao, Bioresour. Technol. 244 (2017) 726–732.